Neutron-proton bremsstrahlung from low-energy heavy-ion reactions

N. Gan, K.-T. Brinkmann, A. L. Caraley, B. J. Fineman, W. J. Kernan,* and R. L. McGrath
Physics Department, State University of New York at Stony Brook, Stony Brook, New York 11794

P. Danielewicz
National Superconducting Cyclotron Laboratory and Department of Physics and Astronomy, Michigan State University, East Lansing, Michigan 48824

(Received 6 May 1993)

High-energy photon yields from the reactions $^{12}C + ^{112,124}Sn$ at 10 MeV/nucleon have been measured. The ratio of cross sections ($E_\gamma \geq 30$ MeV) $\sigma(^{124}Sn)/\sigma(^{112}Sn)$ is 1.6 ± 0.2, which is larger than expected within the equal-participant model. The elementary n-p-γ cross section is evaluated within the neutral scalar σ meson exchange model, and implemented into a BUU code. The results of the BUU calculation suggest that the high-energy γ-ray yield differences for the two Sn isotopes arise from the differences in nucleon phase-space distributions. The sensitivity of the high-energy photon production to the initial phase-space conditions is explored.

PACS number(s): 25.70.−z

I. INTRODUCTION

In the last few years, high-energy photon production ($E_\gamma \geq 30$ MeV) in the intermediate energy region ($E/A > 20$ MeV/nucleon) has been measured systematically [1,2]. Experimental and theoretical studies are consistent in attributing these hard photons to incoherent bremsstrahlung radiated from individual neutron-proton collisions during the early stage of nuclear reactions. Because high-energy photons are only coupled with nucleons by the electromagnetic interaction and have no final state interactions, they can serve as a possible "clean" probe for the collision chronology. Even at energies as low as 10 MeV/nucleon, previous studies [3,4] found similar phenomena. Here the high-energy photon yield exceeds substantially the standard statistical contribution from giant dipole resonance (GDR) decay. The observed forward-backward anisotropy in the laboratory frame, which is expected from a source moving at the half beam-velocity nucleon-nucleon frame, supports the view that high-energy photons from low-energy reactions have the same origin as at higher energies. However, the high-energy photon yield varies with projectile/target combinations more drastically than expected from the scaling relation [5,6] used at higher incident energies. Based on a simple geometrical overlap, equal-participant model, the relation predicts that the high-energy photon yield for different projectile/target combinations should be proportional to the first-chance proton-neutron collisions. The relation does not take into account details of nucleon momentum distributions. Since Pauli blocking constrains high-energy photon production much more severely at lower energies, high-energy photons produced in low-energy reactions may provide a sensitive probe of the nucleon-phase space distributions inside the nucleus. In this paper, we present the results of a new measurement of the inclusive photons in $^{12}C + ^{112,124}Sn$ reactions at 10 MeV/nucleon, and the results of an analysis based on the BUU nuclear transport equation.

II. EXPERIMENT

The experiment was performed at the Stony Brook LINAC. Enriched 3.0 mg/cm^2 self-supporting foil targets of 96.7% ^{124}Sn and 98.9% ^{112}Sn were irradiated with a 120 MeV ^{12}C beam. Photons were detected with a compact BaF_2 array. The whole array was located at 90° with respect to the beam axis, and 25 cm from the target with a 10-cm-diameter lead collimator in front. The array consists of seven 5.6 × 14-cm hexagonal BaF_2 crystals surrounded by a 3-cm-thick NE102 plastic cosmic-ray veto shield. The detector performance was reported in a previous paper [7]. The beam was monitored by recording the ratio of elastic-scattering events detected by two surface-barrier detectors positioned at ±15° with respect to the beam. These elastic events were later used to normalize the data. Two NaI arrays were also positioned in the scattering chamber to detect light charge particles and particle-γ-ray coincidences. The coincidence results will be reported elsewhere.

Good discrimination of high-energy photons from neutrons is a crucial requirement for the high-energy γ-ray detector. Neutrons were rejected by means of pulse-shape discrimination (PSD) deduced from the two components of light output of the BaF_2 scintillator, and by measuring the time-of-flight (TOF) relative to the LINAC RF signal. The overall time resolution was about 900 ps. In Fig. 1, we show the TOF spectra with equivalent photon energy exceeding 30 MeV for the two Sn targets. The

*Present address: EG&G Energy Measurements, Washington Aerial Measurements Department, Suitland, MD 20746.

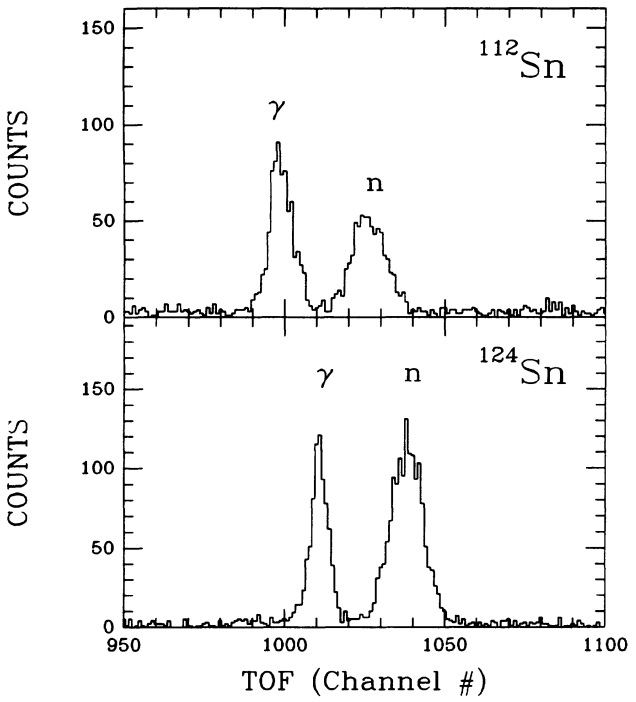

FIG. 1. TOF spectra for events with pulse heights corresponding to $E_\gamma \geq 30$ MeV.

photon and neutron peaks are well-separated, so a simple cut is good enough for the purpose of gating on photons in data analysis.

Effects of pileup on the spectra were considered. The most potentially serious situation would arise from pileup of low-energy evaporated neutrons with γ rays, both because of high multiplicity (CASCADE gives $\langle M_n \rangle \approx 4$ and 8 for ^{112,124}Sn, respectively), and because rejection of such events (where the neutrons generate relatively small scintillation signals), via TOF and/or PSD, could be unreliable. The impact of neutron pileup was assessed in two ways. First, the BaF_2 detector response to neutrons with low energies in the evaporative range was determined using the $^{11}B(p,n)^{11}C$ reaction. A Monte Carlo simulation incorporating the measured response function together with the CASCADE $\langle M_n \rangle$'s shows that pileup causes only a very small spectral distortion. The same conclusion comes from a second simulation which employed the actual pulse-height distribution produced by neutrons emitted in the ^{12}C + Sn reactions. In both cases, the apparent increase in yield of γ rays with $E_\gamma > 30$ MeV due to pileup is less than $\sim 3\%$.

The γ-ray detector array was calibrated using the radiative capture reaction $^{11}B(p,\gamma)^{12}C$ at 7 MeV beam energy, which gives 22.4 MeV and 17.9 MeV γ rays. Inelastic ^{12}C+^{12}C scattering produced 15.1 MeV γ rays which could also be used for calibrations and gain shift checks. The detector response was simulated using the GEANT (version 3.14) code [8].

The unfolded absolute yield of photons was normalized to the elastic cross section at 15°:

$$\frac{d^2\sigma}{d\Omega dE_\gamma} = \frac{\Delta N_\gamma}{\Delta E_\gamma N_{\text{elastic}}} \frac{\Delta\Omega_{\text{elastic}}}{\Delta\Omega_\gamma} \left(\frac{d\sigma}{d\Omega}\right)_{\text{elastic}} . \quad (1)$$

The elastic cross sections were measured in a separate experiment. The absolute elastic cross section is about 10% higher than the Rutherford cross section at 15°. The elastic cross section ratio for the targets is found to be 1.03 ± 0.10. In the discussion below, instead of deconvoluting the data, the calculations are folded with the GEANT calculated response function and compared with the data. To check how well the detector efficiency can be reproduced by GEANT, data are compared in Fig. 2 to a CASCADE [9] calculation folded with the calculated response function. The full dipole sum-rule strength was used for GDR decay. Since the fusion cross section σ_{fus} has not been measured for these reactions, we estimated σ_{fus} to be 1400 mb and 1480 mb for ^{12}C on ^{112}Sn and ^{124}Sn respectively from published data on similar reactions [10] and the extra-push model. The other parameters used in the CASCADE calculation are the same as given in Ref. [3]. The light charged particle yield (not shown) predicted by the same calculation with standard parameters is fitted within 10% to the measured cross section. After folding, the CASCADE results are systematically 20% lower than the γ spectra for both targets. Therefore an overall common normalization factor 1.25 was applied to the calculations.

The γ-ray spectra and relative yields are comparable

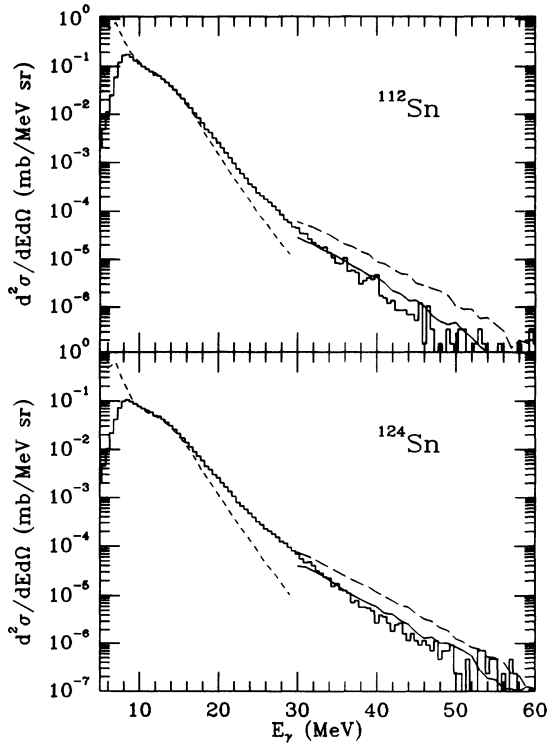

FIG. 2. γ-ray spectra for the reactions ^{12}C + ^{112,124}Sn at 120 MeV. The histograms show the unfolded experimental data. The short-dashed lines are the CASCADE calculations. The solid lines represent the BUU calculations with diffuse nuclei in Thomas-Fermi approximation. The long-dashed lines represent the BUU calculations assuming sharp sphere nuclei. All the calculations are folded with the GEANT calculations. The irregularities in the curves are due to the statistical fluctuations in the Monte Carlo computations.

with those observed in Ref. [3]. For example, in the GDR region (10 to 15 MeV), the ratio of ^{112,124}Sn yields is 1.37 compared to 1.35. For $E_\gamma > 20$ MeV, the ratio is 0.87 compared to 0.90.

III. THEORETICAL CALCULATION

The dynamics of nuclear collisions can be described in terms of the evolution of the one-body distribution function in phase space, as modeled by the Boltzmann-Uehling-Uhlenbeck (BUU) equation [11]. The Monte Carlo BUU code used here has been successfully applied to composite particle and pion production in higher-energy heavy-ion reactions [12,13]. Since isospin is treated explicitly, this code is appropriate for the studies of neutron-proton bremsstrahlung from reactions with different projectile/target combinations. In the program, the nuclear medium correction for the nucleon-nucleon cross section is also taken into account [14]. The γ-ray production probability was implemented in the program for present applications. Because the probability of producing γ-rays per n-p collision is small ($\sim 10^{-5}$), it can be calculated perturbatively without changing the flow of nucleons in phase space. The total γ-ray cross section is obtained by integrating photons generated in each of the individual neutron-proton collisions over time, and then over impact parameter.

The elementary probability for neutron-proton bremsstrahlung is calculated using the neutral scalar σ meson exchange model, with mass m_σ=428 MeV, in the nucleon-nucleon center-of-mass system by standard QFT (quantum field theory) methods [1]. Compared with the semiclassical bremsstrahlung method [15], the approach used here takes into account the 3-body final state phase space, the effect of the emitted γ-ray on the nucleon part of the matrix element, and the spin of the nucleon. Figure 3 illustrates that for energies much lower than the kinematic limit for γ-ray production, the quantum neutral σ meson exchange model and the semiclassical bremsstrahlung model are in good agreement. However, near the kinematic limit, which is the interesting region here, the semiclassical bremsstrahlung model overpredicts the photon yield drastically. In the actual BUU calculation, the quantum calculation is fitted by an analytical expression:

$$\frac{d^2P_\gamma}{d\Omega dE} = 1.671 \times 10^{-7} \frac{(1-x^2)^\alpha}{x} (\mathrm{MeV}^{-1}), \qquad (2)$$

where

$$x = \frac{E_\gamma}{E_{\max}}, \qquad (3)$$

$$\alpha = 0.7319 - 0.5898\beta, \qquad (4)$$

$\beta = v/c$ is the nucleon velocity, and $E_{\max}$ is the total available energy in the nucleon-nucleon center-of-mass system. Photons are assumed to be emitted isotropically in the nucleon-nucleon center-of-mass frame, therefore the photon probability is averaged over the solid angle of 4π. The BUU predicted yield for $E_\gamma \geq 30$ MeV, using the quantum formula, is reduced by about 50% compared to the result using the semiclassical expression.

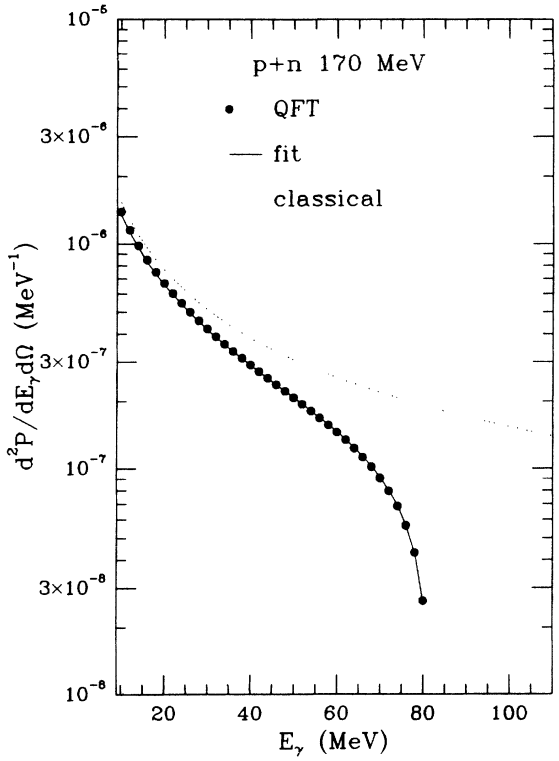

FIG. 3. Angle-averaged probability of neutron-proton bremsstrahlung per n-p collision at 170 MeV proton energy in the lab frame. The classical bremsstrahlung calculation (dotted line), the quantum neutral σ meson exchange model calculation (points), and the analytical function fitting the quantum calculation given in the text (solid line) are shown.

Figure 4 shows the high-energy γ-ray source distribution of nucleon momenta along the beam direction for a central ^{12}C + ^{124}Sn collision at 10 MeV/nucleon calculated with the BUU code. This clearly shows that photons are emitted in collisions initiated from the "end-caps" of the momentum distribution. At such low beam energy, the only way to generate these high-energy photons is by the "Fermi boost" coming from the intrinsic motion of the nucleons. After the photons are emitted, the nucleons will populate the region at $P_z \approx 0$, which is Pauli blocked in the simple two-Fermi sphere model [3]. In the dynamical evolution of the collision, the nucleon redistribution makes room for $P_z \approx 0$ final states. As expected, most of the high-energy photons are emitted in the early phase of the collisions ($\sim$ 80% in 4×10^{-22} s). These features are qualitatively similar to those of calculations applied at higher energies as shown, for example, by Cassing *et al.* [1].

As a comparison to other work, we have calculated photon-photon yields for the 15 MeV/nucleon ^{16}O $+^{\mathrm{nat}}$W reaction. We find for $E_\gamma \geq 30$ MeV a cross section and slope parameter of 15 μb and 5.5 MeV, respectively. The measured values are 10.5$\pm$0.5 μb and 5.8$\pm$0.5 MeV [16]. Our results are quite similar to those given

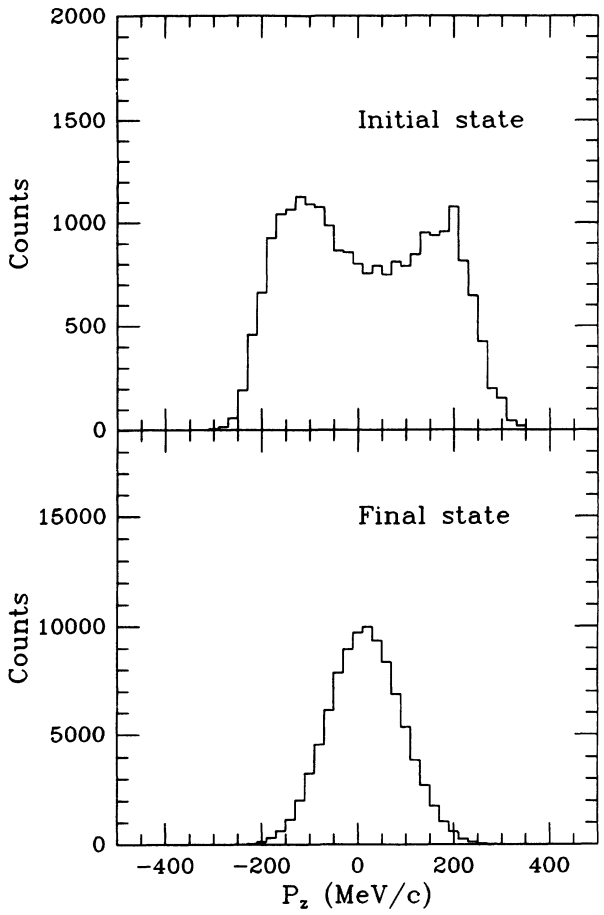

FIG. 4. The top and bottom panels show the initial and final momentum distributions of nucleons involved in the production of high-energy photons with $E_\gamma \geq 30$ MeV for a central $^{12}C + ^{124}Sn$ collision at 10 MeV/nucleon according to the BUU calculation. The distributions are presented in the nucleus-nucleus center-of-mass frame.

by Cassing *et al.* [1] for this low-energy reaction. Other parametrizations of the p-n-γ process may be more appropriate at energies above about 25 MeV/nucleon as discussed in Ref. [1], and by Nakayama [17].

IV. DATA ANALYSIS AND RESULTS

The total high-energy γ-ray cross section ($E_\gamma \geq 30$ MeV) is 4.3 μb and 6.9 μb for ^{112}Sn and ^{124}Sn, respectively. Because of the uncertainty of the efficiency, the systematic error on the absolute cross section is estimated to be about $\pm 30\%$, although the relative yields are more accurately determined. The slope parameter is 4.0 ± 0.2 MeV. The simple systematics deduced from intermediate energies [1] would give a photon production cross section of only 0.28 μb, about one order of magnitude lower than measured. On the other hand, the slope parameters from the same systematics agree with our findings. The situation with respect to the systematics and the data is similar to that reported in the low-energy studies on C + Mo reactions in Ref. [4].

In Ref. [3], the cross section ratio of high-energy photons, $R = \sigma(^{124}Sn)/\sigma(^{112}Sn)$, was reported to be $1.8^{+0.7}_{-0.4}$ for $E_\gamma \geq 20$ MeV, after subtracting the calculated statistical component from the experiment data. In the present measurement, for $E_\gamma \geq 30$ MeV, the statistical component is suppressed about 2 or 3 orders of magnitude compared with the nonstatistical component. Therefore the uncertainty introduced by the statistical-model calculations is avoided. For these high-energy γ rays, the ratio $R = 1.6 \pm 0.2$. A pronounced target effect is confirmed. The cross section ratio deviates from the equal-participant model scaling prediction of 1.1.

In Fig. 2, the comparison between the BUU simulation folded with the detector response function and the data is shown. The total high-energy photon cross sections ($E_\gamma \geq 30$ MeV) predicted by BUU, 4.4, and 6.4 μb for ^{112}Sn, and ^{124}Sn respectively, are in fairly good agreement with the experiment. Possible sources of discrepancy could be due to the uncertainty in the absolute detector efficiency, and the n-p-γ probability in the theoretical calculation. The calculated slope parameter is 5.1 ± 0.1 MeV, which is about 25% higher than measured.

In the region $E_{\rm beam}/A \approx 10$ MeV, the relative velocity of the nuclei is much smaller than the Fermi velocity, so the subtle interplay between the Fermi boost and Pauli blocking is expected to strongly affect the γ-ray production. In the simple equal-participant model, the nucleon distributions in phase space are not taken into account explicitly. For the more realistic BUU calculation, the initial density distributions of neutrons and protons in configuration space are obtained by minimizing the total energy of the nucleus, which is a functional of proton and neutron configuration space density in the Thomas-Fermi approximation [18,19]. The momentum distributions are then deduced by distributing neutrons and protons randomly according to their Fermi momentum, which is related to the density distribution $\rho(r)$ in configuration space by the local Thomas-Fermi (LTF)relation:

$$k_f(r) = [3\pi^2 \rho(r)]^{\frac{1}{3}}. \quad (5)$$

In Fig. 5, the initial space and momentum distributions of neutrons for both Sn nuclei are shown (for protons, the distributions are similar for both Sn isotopes, as expected). Since there are more high-momentum neutrons in the ^{124}Sn nucleus than in the ^{112}Sn nucleus, more high-energy photons are generated. The model calculation, after averaging over impact parameter, yields the ratio $R = 1.45 \pm 0.05$, which is consistent with the experimental data.

To illustrate the sensitivity of hard photon production to the initial phase space distributions, a sharp sphere approximation was also tried. The root-mean-square radius of the sharp nucleus is taken equal to that of the diffuse nucleus in the Thomas-Fermi approximation, as shown in Fig. 5. As can be seen in Fig. 2, the predicted photon yields employing the sharp sphere distributions are larger and less compatible with the data than the more realistic Thomas-Fermi prediction. The sharp nucleus approximation gives relatively more nucleons in the high-momentum region, and thus enhances the high-

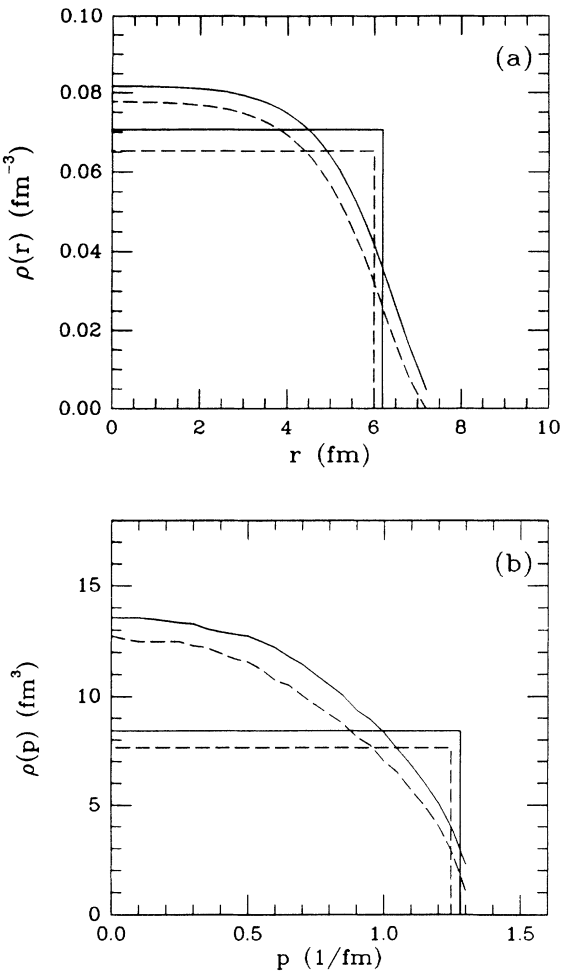

FIG. 5. (a) shows the space distributions of neutrons for ^{112}Sn (dashed line) and ^{124}Sn (solid line) in both Thomas-Fermi and sharp sphere approximations. The rms radii were kept the same in both approximations. (b) shows the associated momentum distributions obtained by the local Thomas-Fermi relation.

energy photon yield. This approximation results in a reduced isotope ratio R of 1.25 ± 0.05. Compared to the Thomas-Fermi approximation, in the high-momentum region ($p > 0.9$ fm^{-1}), which is important for photon production, the proton ratio between ^{124}Sn and ^{112}Sn decreases from 0.97 to 0.85, and the neutron ratio decreases from 1.2 to 1.1. The combination of these two effects causes the reduction of R.

At these very low incident energies, high-energy photons provide information on nucleon phase-space distributions (especially momentum) that may be obscured at higher energies. For example, for the reactions studied here, the BUU calculations in Thomas-Fermi approximation predict the ratio to be only 1.10 ± 0.05 at 60 MeV/nucleon, more like the scaling expectation.

V. SUMMARY

In summary, we have measured high-energy photon production in the reactions ^{12}C + ^{112,124}Sn at 10 MeV/nucleon. The measured cross section ratio is 1.6 ± 0.2 for $E_\gamma \geq 30$ MeV. The n-p-γ elementary cross section is calculated from the neutral σ-meson exchange model and is implemented into a BUU dynamical calculation. The calculation shows that the high-energy photons are emitted in the very early stage of the reaction, and preferentially from the high momentum component of the nucleon momentum distribution. By modeling the dynamical evolution of the nucleon phase space carefully, the calculations reproduce the experimental data quite well, and indicate that the isotope effect of high-energy photon yields originates from differences in the nucleon phase-space distributions. These very low-energy heavy-ion collisions appear to offer a sensitivity to the high-momentum components of the nucleon distribution. For example, 50 MeV photons correspond to nucleon momenta ≈ 200 MeV/c. The present results show that the incoherent nucleon-nucleon bremsstrahlung mechanism is dominant in the γ-ray energy range observed in this work. For somewhat higher photon energies, it would be interesting to search for evidence of the competitive coherent nucleus-nucleus bremsstrahlung process, with its distinctive dipole effective charge signature [5,20].

ACKNOWLEDGMENTS

The authors wish to thank J.A. Alexander and E. Bauge for their helpful discussions. We are also indebted to the technical staff at Stony Brook for the accelerator operation. This work was supported in part by the U.S. National Science Foundation.

[1] W. Cassing, V. Metag, U. Mosel, and K. Niita, Phys. Rep. 188, **No 6**, 363 (1990).
[2] H. Nifenecker and J.A. Pinston, Ann. Rev. Nucl. Part. Sci. **40**, 113 (1990); H. Nifenecker and J.A. Pinston, Prog. Part. Nucl. **23**, 271 (1989).
[3] R.J. Vojtech, R. Butsch, V.M. Datar, M.G. Herman, R.L. McGrath, P. Paul, and M. Thoennessen, Phys. Rev. C **40**, R2441 (1989).
[4] C.A. Gossett, J.A. Behr, S.J. Luke, B.T. McLain, D.P. Rosenzweig, and K.A. Snover, Phys. Rev. C **42**, R1800 (1990).
[5] H. Nifenecker and J.P Bondorf, Nucl. Phys. **A442**, 478 (1985).
[6] H. Bertholet, M. Kwato Njock, M. Maurel, E. Monnand, H. Nifenecker, J.A. Pinston, F. Schussler, D. Barneoud, C. Guet, and Y. Schutz, Nucl. Phys. **A474**, 541 (1987).
[7] W.J. Kernan, N. Gan, A.L. Caraley, B.J. Fineman, R.L. McGrath, and R.J. Vojtech, Nucl. Instrum. Methods **A313**, 563 (1992).
[8] R. Brun *et al.*, GEANT3 User's Guide (CERN, DD/EE/84-1, 1987).
[9] F. Pühlhofer, Nucl. Phys. **A280**, 267 (1977).

[10] I. Tserruya, V. Steiner, A. Fraenkel, P. Jacobs, D.G. Kovar, W. Henning, M.F. Vineyard, and B.G. Glagola, Phys. Rev. Lett. **60**, 14 (1988).
[11] G.F. Bertsch and S. Das Gupta, Phys. Rep. **160** (4), 189 (1988).
[12] P. Danielewicz and G. F. Bertsch, Nucl. Phys. **A533**, 712 (1991).
[13] P. Danielewicz and Q. Pan, Phys. Rev. C **46**, 2002 (1992).
[14] A. Lejeune, P. Grange, M. Marizolff, and J. Cugnon, Nucl. Phys. **A453**, 189 (1986).
[15] J.D. Jackson, *Classical Electrodynamics* (Wiley, New York, 1975), p. 702.
[16] G. Breitbach, G. Koch, S. Koch, W. Kühn, A. Ruckelshausen, V. Metag, R. Novotny, S. Riess, D. Habs, D. Schwalm, E. Grosse, and H. Ströher, Phy. Rev. C **40**, 2893 (1989).
[17] K. Nakayama, Phys. Rev. C **42**, 1009 (1989).
[18] A.N. Antonov, P.E. Hodgson, and I. Zh. Petkov, *Nucleon Momentum and Density Distributions in Nuclei* (Oxford University Press, New York, 1988)
[19] R.J. Lenk and V.R. Pandharipande, Phys. Rev. C **39**, 2242 (1989).
[20] K. Nakayama and G.F. Bertsch, Phys. Rev. C **36**, 1848 (1987).